의학박사 학위논문

췌장선암 정맥침범 마커로서의 TIMP1

TIMP1 as venous invasion marker in pancreatic ductal adenocarcinoma

울 산 대 학 교 대 학 원

의 학 과

성 유 나

췌장선암 정맥침범 마커로서의 TIMP1

지도교수 홍 승 모

이 논문을 의학박사 학위 논문으로 제출함

2023 년 8 월

울 산 대 학 교 대 학 원

의 학 과

성 유 나

성유나의 의학박사학위 논문을 인준함

심사위원 장 성 욱 인

심사위원 송 태 준 인

심사위원 송 기 병 인

심사위원 전 선 영 인

심사위원 홍 승 모 인

울 산 대 학 교 대 학 원

2023 년 8 월

Abstract

Background

Pancreatic ductal adenocarcinoma (PDAC) is the 8th most common cancer in Korea and has a low 5-year overall survival rate (YSR) of about 12.2%. Although venous invasion is known to be the cause of poor prognosis, the precise mechanism is still unknown. In this study, we investigated biomarkers involved in venous invasion and their mechanisms using gene expression arrays and functional validation.

Materials and methods

Eight surgically resected formalin-fixed, paraffin-embedded (FFPE) PDAC tissues were collected. Meticulous manual microdissections for gene expression arrays were performed on the following three groups. 1) portal vein/ superior mesenteric vein with cancer cell invasion (VI); 2) pancreatic cancer without portal vein/ superior mesenteric vein invasion (CA); and 3) normal portal vein/ superior mesenteric vein tissue (NV). The candidate gene expressions were validated at protein level in 220 cases using 2D images with immunohistochemistry (IHC) and 3D images with tissue clearing and multiple immunofluorescence labeling. To identify the role of potential biomarker in venous invasion, invasion assay and western blot analysis were performed using human endothelial (EA.hy926), cancer-associated fibroblast (CAF), and pancreatic cancer (Panc1) cell lines.

Results

Four genes, includingTIMP1, CXCR4, OLFML2B, and CYP1B1, were specifically expressed in VI group. TIMP1 ($p = 0.026$) and CXCR4 protein ($p < 0.001$) expression in VI set were significantly higher than in CA set. Specific TIMP1 expression in venous invasive areas was found by 3D imaging. The patients with strong TIMP1-expression more commonly had lymphovascular invasion ($p <$

0.001) and low 5-YSR (p = 0.027) than those with weak TIMP1-expression. TIMP1 inhibition by siRNA reduced cancer cell invasion ability in the presence of CAF. TIMP1 was increased in pancreatic cancer cells along with PI3Kp110 and phospho-AKT in co-culture conditions mimicking venous invasion.

Conclusions

TIMP1 was a potential biomarker of venous invasion in PDAC and the TIMP1/PI3K/Akt signaling pathway may be involved. This could provide basic information for development of inhibitors to prevent venous invasion in patients with PDAC.

Keywords: Venous invasion; Pancreatic cancer; Biomarker; TIMP1

Contents

Abstract ····· i

Contents ····· iii

List of Table ····· v

List of Figures ····· vi

Introduction ····· 1

Materials and Methods ····· 3

1. Case selection ····· 3
2. Gene expression array using NanoString ····· 3
3. Tissue microarray (TMA) for IHC validation ····· 4
4. Immunohistochemistry····· 4
5. Tissue immunolabeling and 3D imaging ····· 5
6. Cell culture ····· 5
7. siRNA transfection ····· 6
8. Cancer cell invasion assay ····· 6
9. Western blot analysis ····· 7
10. Statistical analysis ····· 7

Results ····· 9

1. Clinicopathologic characteristics ····· 9
2. Candidate genes for venous invasion through Nanostring gene expression assay ····· 9

3. Protein expression of TIMP1 and CXCR4 genes ····· 9

4. Association between TIMP1 and CXCR4 in cell migration and invasion ····· 10

5. The effect on TIMP1 in venous invasion ability of pancreatic cancer cell line ····· 11

6. The association of TIMP1 expression of pancreatic cancer cell with TIMP1/PI3K/Akt signaling in venous invasion ·11

Discussion ····· 29

References ····· 32

Korean Abstract ····· 38

List of Table

Table 1. Clinicopathologic characteristics of cases used in this study ·····12

Table 2. Clinicopathologic factors according to TIMP1 expression status ·····13

Table 3. Clinicopathologic factors according to CXCR4 expression status ·····14

List of Figures

Figure 1. Representative image of uncovered hematoxylin and eosin-stained slide for manual microdissection ·····15

Figure 2. Scatter plot showing gene expression fold change of vascular invasion group (VI) compared to cancer (CA) and normal vessel (NV) group ·····16

Figure 3. Representative images of portal/ superior mesenteric vein with cancer invasion ····· 17

Figure 4. TIMP1 immunohistochemical sections with different intensity ·····18

Figure 5. Number of strong TIMP1 expression cases in VI and CA set ·····19

Figure 6. Overall survival according to TIMP1 status ·····20

Figure 7. CXCR4 immunohistochemical sections with different score ·····21

Figure 8. Number of cases for each CXCR4 immune-score in VI and CA set ·····22

Figure 9. Boxplot of CXCR4 immune-score in CA and VI set ·····23

Figure 10. Overall survival according to CXCR4 expression status ·····24

Figure 11. Representative image of multicolor immunofluorescent labeling of pancreatic ductal adenocarcinoma tissue with vascular invasion ·····25

Figure 12. Scatter plot showing association between CXCR4 (tumor, stroma, and inflammatory cells) and TIMP1 using immune-score ·····26

Figure 13. Invasion ability assay by boyden chamber system ·····27

Figure 14. Western blot analysis in co-culture condition ·····28

Introduction

Pancreatic ductal adenocarcinoma (PDAC) is the 8th most common cancer in Korea and has a low 5-year overall survival rate of about 12.2% (1). Factors known to influence the prognosis of PDAC include venous invasion as well as perineural invasion, lymph node metastasis, and resection marginal status (2-7). Among them, large vein invasion, such as the portal vein or superior mesenteric vein, is frequently found in PDAC due to its anatomical proximity. Large vein invasion of PDAC may cause rapid hepatic metastasis via portal vein, resulting in a poor prognosis for patients (8-11).

According to meta-analysis of PDAC, the frequency of vascular invasion in patients who underwent surgery is about 49%(12). The terms 'lymphovascular invasion' or 'microvascular invasion' are used interchangeably in different studies because it is challenging to differentiate between capillary and lymphatics without a muscle layer. While the vascular network is composed continuously, lymphovascular invasion can be classified into 'microvascular invasion' or 'large vessels invasion' depending on the presence or absence of thick smooth muscle layer. In case of large vessel invasion, cancer cells have higher aggressiveness to penetrate the thick muscle layer and are closer to hepatic metastasis through venous drainage, suggesting a worse prognosis than microvascular invasion. At this time, it has been reported that when tumor cells completely encircle or destructs a venous wall during large vessel invasion, CD31 or desmin IHC increases the venous invasion detection rate(13). Given the above underestimation in detecting venous invasion, the actual venous invasion rate is expected to be higher in PDAC, and since the venous invasion is an independent predictor of poor prognosis in PDAC, it is very important to understand the precise mechanism related to large vessel invasion in PDAC(14)

When the venous invasion process in PDAC was observed in three-dimensional context using cleared tissue, it became apparent that invasion could occur while preserving the glandular structure, rather than in the form of a single discohesive

cell(15). Additionally, the result of E-cadherin staining proposed that EMT was not sustained(15). However, a more specific mechanism related to venous invasion remains unknown. Several studies have investigated gene expression patterns associated with vascular invasion in different organs, including the liver, breast, and uterus (16-20). Most of the studies, including TCGA data (16, 17, 19, 20), found genes related to vascular invasion through comparisons between cancers with and without pathologic information of vascular invasion. However, it would be beneficial to comprehend the molecular mechanism of venous invasion in PDAC by comparing cancer tissues with and without actual lesions of venous invasion.

Considering that the venous invasion rate in PDAC patients is about 88%(15), which is higher than cancers of other abdominal organs, and that such venous invasion is involved in systemic metastasis and poor prognosis, understanding the molecular mechanism of venous wall invasion is an important step to improve the patient's prognosis through future therapeutic target development. Therefore, in this study, we aimed to find candidate genes involved in large venous wall invasion in PDAC by gene expression array through micro-dissected tissues specific to venous wall invasion. In addition, the protein expression validation of candidate genes was performed.

Materials and methods

Case selection

This study was performed after approval from the Institutional Review Board (approval number: 2020-0234) with a waiver of the informed consent. Cases for gene expression array and protein validation were collected from the records of the Department of Pathology at the Asan Medical center, University of Ulsan College of Medicine from 2005 to 2014.

Gene expression array using NanoString

The gene expression array was performed using NanoString. A total of 8 cases in the NanoString set was divided into the following 3 groups, and manual microdissection of formalin-fixed, paraffin-embedded (FFPE) tissues was performed guided by hematoxylin and eosin-stained slides. 1) Portal/ superior mesenteric vein with cancer invasion (VI); 2) Cancer without portal/ superior mesenteric vein involvement (CA); 3) Normal portal/ superior mesenteric vein (NV). RNA was extracted using FFPE RNeasy kit (Qiagen, Hilden, Germany) and quality was measured by Agilent BioAnalyzer 2100 (Agilent Technologies, Santa Clara, CA, USA) according to the manufacture's protocol. Twenty-four RNA samples (matched 8 VI, 8 CA and 8 NV from each patient) were used for gene expression assay using PanCancer Progression panel of NanoString with 770 probes containing 730 cancer- related and 40 housekeeping genes (NanoString Technologies, Seattle, WA, USA). RNA (250-1200 ng) was hybridized with probes and RNA transcripts number were counted by NanoString nCounter Digital Analyzer (NanoString Technologies, Seattle, WA, USA). The raw data was normalized and analyzed using nSolver Analysis software (NanoString Technologies, Seattle, WA, USA).

Tissue microarray (TMA) for IHC validation

The validation for protein expression was performed in an independent cohort, consisting of 205 PDACs without portal/ superior mesenteric vein involvement (CA) and 15 PDACs containing foci of portal /superior mesenteric vein invasion set (VI). Tissue microarrays (TMAs) were constructed from FFPE PDAC tissue blocks using a manual tissue micro-arrayer (Uni TMA Co, Ltd, Seoul, Korea). Selection criteria included areas with >75% of tumor cells, and no tumor necrosis. TMAs for the CA set and VI set were constructed separately. For the CA set, 2-mm diameter punches were used to extract four representative PDAC tissue cores from a donor block and transfer them into a new recipient block along with one core from a matched normal pancreas tissue. For the VI set, a 4.5mm diameter punch was used to transfer a representative portal/ superior mesenteric vein with cancer invasion from a donor block and transfer it to a new recipient block.

Immunohistochemistry

IHC was performed on 4-μm-tick sections using a Ventana auto-stainer and an ultra-View DAB Detection Kit (Ventana, Tucson, Arizona) as per the manufacturer's instructions, on representative lesions from FFPE tissues. Primary antibodies for TIMP1 (clone EPR18352, abcam, UK, Cambridge, 1:500, Rabbit monoclonal) and CXCR4 (clone UMB2, abcam, UK, Cambridge, 1:2000, Rabbit monoclonal) were used. For TIMP1, the intensity was scored based on the highest cytoplasmic intensity as follows: 0, negative staining; 1, weak staining; 2, intermediate staining; 3, strong staining. However, if the area occupied was less than 5%, it was evaluated as 0 regardless of intensity. For CXCR4 IHC, the immunohistochemical score (IS) was calculated by multiplying the nuclear intensity (0: negative; 1: weak, staining contour not visible at x40, but visible at x100; 2: strong, staining contour distinct at x40) and the fraction (0: 0%; 1: <1/3;

2: 1/3 ~ 2/3; 3: >2/3) of expressing tumor cells. If possible, stromal cells or inflammatory cells assessed in a similar manner to tumor cells.

Tissue immunolabeling and 3D imaging

Tissue immunolabeling and 3D imaging was performed as previously described (15, 21). In brief, PDAC tissues were incubated and washed with PBS/0.2% Tween-20 with 10 mg/mL heparin. Primary antibodies, including cytokeratin 19 (EP1580Y, rabbit monoclonal; 1:200; Abcam, Cambridge, UK), desmin (goat polyclonal; 1:100, LifeSpan Biosciences, Seattle, WA, USA), and TIMP1 (F31P2A5, mouse monoclonal; 1:200; invitrogen, CA) were used. Following primary antibody labeling, a number of steps including washing, secondary antibody incubation, centrifugation, and sonication of tissues were performed. Then the tissue was dehydrated with serially concentrated methanol, incubated and transferred to dibenzyl ether (DBE) overnight. A confocal laser scanning microscope (LSM800; Carl Zeiss, Jena, Germany) was used to visualize immunolabeled tissue structures in 3D. A bandpass filter set with an excitation range of 480/40 nm and an emission range of 525/50 nm was used to see the Alexa 488 signals of epithelial cells, both normal ductal cells and cancer cells that express the cytokeratin 9. A filter set with an excitation range of 400/40 nm and an emission range of 421/50 nm was used to see the DyLight 405 signals of desmin-expressing smooth muscle cells. And filter set with an excitation range of 550/40 nm and an emission range of 570/50 nm was used to see the Alexa 488 signals of TIMP1-expressing tumor cells. 3D images were generated with IMARIS software (Version 9.4, Bitplane, Zurich, Switzerland).

Cell culture

Human pancreatic ductal cancer cell line, Panc1, was provided by Dr. J.K Ryu and cultured with Dulbecco's modified Eagle's medium (DMEM, GIBCO, Waltham, MA).

Human endothelial cell line, EA.hy926 obtained from the American Type Culture Collection (ATCC, Manassas, VA) maintained with DMEM. RPMI-1640 culture medium (Gibco, Waltham, MA) was used to culture human pancreatic cancer associated fibroblast (CAF) that was isolated from primary pancreatic cancer cells. These cell lines were grown with media containing 10% (v/v) fetal bovine serum (FBS, Wellgene, Gyeongsan, Korea), penicillin (100 U/mL, Gibco) and streptomycin (100μg/mL, Gibco) at 37 °C in a humidified atmosphere with 5% CO_2. Pancreatic cancer cells, endothelial cells, and CAF were indirectly co-cultured using a culture insert (SPL, Pocheon, Republic of Korea) to create a vascular invasion mimicking environment. $1x10^6$ cells were seeded in 100 mm dish and other $5x10^5$ cells/type were co-cultured using insert with 8.0 μm pore at indicated time.

siRNA transfection

Human TIMP1 siRNA was purchased from Ambion (Thermo Fisher Scientific, Waltham, MA, USA). Panc1 cells were transfected with siRNA for 48 h by oligofectamin according to the manufacture's protocol (Invitrogen, Waltham, MA, USA). Panc1 cells (2 x 105 cells) were transfected with 0.2 μM siRNA/oligofectamine complex in media without FBS at 37°C for 4h, then FBS was added for final 10% concentration. After 48h, Panc1 cells were used for invasion assay or western blot analysis to determine the TIMP1 effect on venous invasive ability of cancer cells. The corresponding target sequence of siRNA are shown as following: TIMP1, 5′-GAUGUAUAAAGGGUUCCAA-3′ and scramble, 5′-UUCUCCGAACGUGUCACGU-3′.

Cancer cell invasion assay

The capacity of cancer cell invasion was assessed using the Boyden chamber system with extracellular matrix (ECM) coated insert in 24-welll plate. Upper chamber with 8.0 μm pore were coated with VitroGel hydrogel matrix (TheWell

Bioscience, North Brunswick, NJ, USA) at 37°C for 20 min and then $1x10^5$ EA.hy926 cells were seeded in upper chamber for 6h. Then, fibroblasts ($1x10^5$ cells/insert) were cultured in the upper chamber for overnight. Pancreatic cancer cells ($2x10^5$ cells/insert) with or without siRNA transfection (for negative control) were incubated to upper chamber with serum free media, while media containing 10% FBS were added in lower chamber. After 24 hours, invasive cancer cells were penetrated through the matrix and chemo-attached to the film at the bottom of the upper chamber. Cotton swabs were gently rubbed against the interior of the upper chamber to remove non-invasive cells. Cell stain solution (Milipore, Darmstadt, Germany) was used to stain invasive cells and 10% acetic acid was used to dissolve them. Cancer cell invasiveness was assessed colorimetrically by ELISA at 560 nm. All experiments were performed in triplicate.

Western blot analysis

SDS-PAGE was used to separate the whole cell protein from cell lines, and then transferred to nitrocellulose membrane (Hybond-ECL, GE Healthcare, Chicago, IL, USA). The membrane was incubated with primary antibody, followed by secondary antibody conjugated with horseradish peroxidase. Specific antigen–antibody complexes were detected by enhanced chemiluminescence (PerkinElmer, Life science). Western blot analysis was performed with the following antibodies: anti-TIMP1 antibody (Invitrogen, CA), anti-Akt, phospho-Akt (p-Akt, S473), Erk1/2, phospho-Erk1/2 (Thr202/Tyr204), PI3Kp110 antibodies (Cell Signaling Technology, MA), and anti-GAPDH antibody as loading control (Santa Cruz Biotechnology, Dallas, TX, USA). Secondary antibodies were obtained from AbClon (Seoul, Republic of Korea).

Statistical analysis

The R software (version 4.02 Vienna, Austria) was used to perform statistical

analyses. The relationship between each clinicopathologic parameter and the TIMP1 or CXCR4 protein expression was investigated with the chi-square test or the Student's t-test. The quantitative relationship between TIMP1 and CXCR4 expression was compared with the Corrgram vesion 1.14. P-values <0.05 were considered as statistically significant.

Results

Clinicopathologic characteristics

The clinicopathologic characteristics of all cases, which were for the gene expression array (n = 8) and for validation (n = 220), are summarized in **Table 1**. The mean age of the patients was 63.4 ± 10.6 years with a male to female ratio of 1.32. A total of 14 tumors (6.1%) were well differentiated, 179 (78.5%) moderately differentiated, and 35 (15.4%) poorly differentiated. And the tumor size was 3.86 ± 1.96 cm. Lymphovascular and perineural invasion were identified in 99 (43.4%) and 189 (82.9%) cases, respectively. Margin involvement was identified in 55 (24.1%) cases. Based on the 8th edition of AJCC cancer staging scheme, four cases were in T1(1.8%), 24 T2 (10.5%), and 200 T3 (87.7%). According to N category, ninety-three were N0 (40.8%), 104 N1 (45.6%), and 31 N2 (13.6%) tumors, respectively.

Candidate genes for venous invasion through NanoString gene expression assay

When comparing the VI group and the other two groups (CA, NV), the genes that showed a difference of more than two-fold in gene expression level and p-value <0.05 were TIMP1, CXCR4, OLFML2B, and DLFM2B **(Figure 1 and 2)**, and the corresponding genes were selected as candidates for venous invasion biomarkers.

Protein expression of TIMP1 and CXCR4 genes

Through pilot IHC study, TIMP1 and CXCR were chosen as potential venous invasion biomarkers that had their proteins validated (**Figure 3**). Based on the intensity of TIMP1 expression, PDACs were divided into two categories (TIMP1 strong, intensity 2 and 3; TIMP1 weak, intensity 0 and 1, **Figure 4**). The strong

TIMP1-expression rate of VI set was higher (86.7%) than CA set (45.0%, **figure 5**, p = 0.026). Compared with clinicopathologic parameters, PDAC with strong TIMP1-expression group more commonly had lymphovascular invasion than those with weak-TIMP1 expression group (55.6% versus 10.1%, p < 0.001, **Table 2**). PDAC patients with strong TIMP1-expression had a poor 5-year overall survival (8.6%) than those with weak TIMP1-expression (15.4%, p = 0.027, **Figure 6).**

The result of CXCR4 IHC were evaluated using IS (**Figure 7**). As a result, six different ISs in total were generated, with each IS's matching number of instances in the VI / CA set is presented in **Figure 8**. The IS of the VI group (4.73 ± 2.22) for CXCR4 was greater than that of the CA group (1.14 ± 1.48, p < 0.001, **Figure 9**). PDACs were divided into two categories based on the IS of CXCR4 expression (CXCR4 strong, IS ≥3; CXCR4 weak, IS <3), and compared with clinicopathologic parameters (**Table 3**). PDAC with strong CXCR4 expression was older than those with weak expression (p = 0.01, **Table 3**). There was no significant difference in 5-year overall survival according to CXCR4 expression status (**Figure 10,** p = 0.8, CXCR4 strong group; 11.8%, CXCR4 weak group,10.6%)

In addition, a 3D multicolor immunofluorescent labelling image demonstrated the expression of TIMP1 in foci of venous invasion of the PDAC. Cytoplasmic TIMP1 expression was clearly visible in tubule-forming cancer cells inside the muscular venous wall, which was similar to that of the 2D immunohistochemical staining (**Figure 11**).

Association between TIMP1 and CXCR4 in cell migration and invasion

To analyze the association between TIMP1 and CXCR4 in cell migration and invasion, we compared the expression of TIMP1 and CXCR4 in tumor, stroma, and inflammatory cells. As a result, there was no discernible link between TIMP1 and CXCR4 expression among tumor, stroma, and inflammatory, with correlation

coefficients of 0.37, 0.35, and -0.01, respectively (**Figure 12**). We only found a correlation of IS of CXCR4 between tumor, stroma, and inflammatory cells (Correlation coefficients: Tumor- stroma, 0.79; tumor- inflammatory cells, 0.52; stroma- inflammatory cells, 0.53).

The effect on TIMP1 in venous invasion ability of pancreatic cancer cell line

To investigate the influence of TIMP1 on venous invasion capacity, an invasion ability assay was performed using Boyden chamber coated with matrix and EA.hy926 endothelial cell after transfection of Panc1 with TMP1 siRNA. Panc1 cells' ability to invade was reduced by around 1.2-fold when TIMP1 expression was lowered as compared to cells with scrambled siRNA transfected ($p = < 0.01$; **Figure 13A**). However, in the absence of CAF, TIMP1 suppression did not lessen the capacity of cancer cells to invade. Additionally, cancer cell invasion ability increased as the number of CAF increased ($p = < 0.001$; **Figure 13B**).

The association of TIMP1 expression of pancreatic cancer cell with TIMP1/PI3K/Akt signaling pathway in venous invasion

To explore the TIMP1 signaling pathway in pancreatic cancer with venous invasion, Panc1, EA.hy926, and CAF were indirectly co-cultured to mimic microenvironment of venous invasion. As the co-incubation time increased, the expression of TIMP1 in cancer cells increased. Along with increased TIMP1 expression, the PI3Kp110 and phosphorylation of Akt and p42 MAPK expressions were also increased. In contrast, total Akt and p44/42 MAPK expression remained unchanged (**Figure 14**).

Table 1. Clinicopathologic characteristics of cases used in this study

Age (yr)		63.4±10.6
Sex	Male	130 (57.0%)
	Female	98 (43.0%)
Differentiation	WD	14 (6.1%)
	MD	179 (78.5%)
	PD	35 (15.4%)
Size (cm)		3.86±1.96
Lymphovascular invasion	Present	99 (43.4%)
	Absent	129 (56.6%)
Perineural invasion	Present	189 (82.9%)
	Absent	39 (17.1%)
Resection margin status	Involved	55 (24.1%)
	Uninvolved	173 (75.9%)
T category	T1	4 (1.8%)
	T2	24 (10.5%)
	T3	200 (87.7%)
N category	N0	93 (40.8%)
	N1	104 (45.6%)
	N2	31 (13.6%)

Table 2. Clinicopathologic factors according to TIMP1 expression status

		TIMP1 expression		
		Weak (0,1)	**Strong (2,3)**	p-value
Age		63.3±9.65	62.3±10.5	0.55
Sex	Male	47 (59.5%)	46 (51.1%)	0.35
	Female	32 (40.5%)	44 (48.9%)	
Differentiation	WD	9 (7.6%)	3 (3.3%)	
	MD	63 (79.7%)	69 (76.7%)	0.24
	PD	10 (12.7%)	18 (20.0%)	
Size		3.85±2.39	3.92±1.77	0.84
Lymphovascular invasion	Present	8 (10.1%)	50 (55.6%)	**< 0.001**
	Absent	71 (89.9%)	40 (44.4%)	
Perineural invasion	Present	62 (78.5%)	75 (83.3%)	0.54
	Absent	17 (21.5%)	15 (16.7%)	
Resection margin status	Involved	12 (15.4%)	21 (23.6%)	0.26
	Uninvolved	66 (84.6%)	68 (76.4%)	
T category	T1	2 (2.5%)	1 (1.1%)	
	T2	5 (6.3%)	2 (2.2%)	0.31
	T3	72 (91.1%)	87 (96.7%)	
N category	N0	39 (49.4%)	37 (41.1%)	
	N1	35 (44.3%)	44 (48.9%)	0.47
	N2	5 (6.3%)	9 (10%)	

Table 3. Clinicopathologic factors according to CXCR4 expression status

		CXCR4 expression		
		Weak (IS<3)	**Strong (IS≥3)**	p-value
Age		62.4±9.81	68.59±8.37	**0.01**
Sex	Male	83 (55.3%)	12 (70.6%)	0.35
	Female	67 (44.7%)	5 (29.4%)	
Differentiation	WD	6 (4.0%)	1 (5.9%)	
	MD	120 (80.0%)	14 (82.4%)	0.85
	PD	24 (16.0%)	2 (11.8%)	
Size		3.87±1.87	4.40±2.43	0.29
Lymphovascular invasion	Present	62 (41.3%)	6 (35.3%)	0.83
	Absent	88 (58.7%)	11 (64.7%)	
Perineural invasion	Present	127 (84.7%)	13 (76.5%)	0.60
	Absent	23 (15.3%)	4 (23.5%)	
Resection margin status	Involved	29 (19.6%)	3 (17.6%)	1.00
	Uninvolved	119 (80.4%)	14 (82.4%)	
T category	T1	1 (0.7%)	1 (5.9%)	
	T2	4 (2.7%)	0 (0%)	0.14
	T3	145 (96.7%)	16 (94.1%)	
N category	N0	63 (42.0%)	7 (41.2%)	
	N1	67 (44.7%)	7 (41.2%)	0.88
	N2	20 (13.3%)	3 (17.6%)	

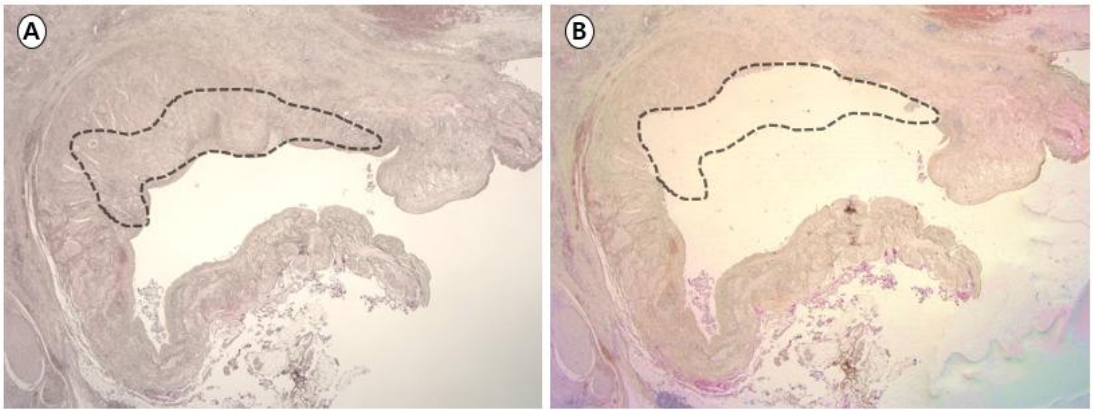

Figure 1. Representative image of uncovered hematoxylin and eosin-stained slide for manual microdissection. Portal/ superior mesenteric vein with cancer invasion area (dashed) before **(A)** and after **(B)** manual microdissection.

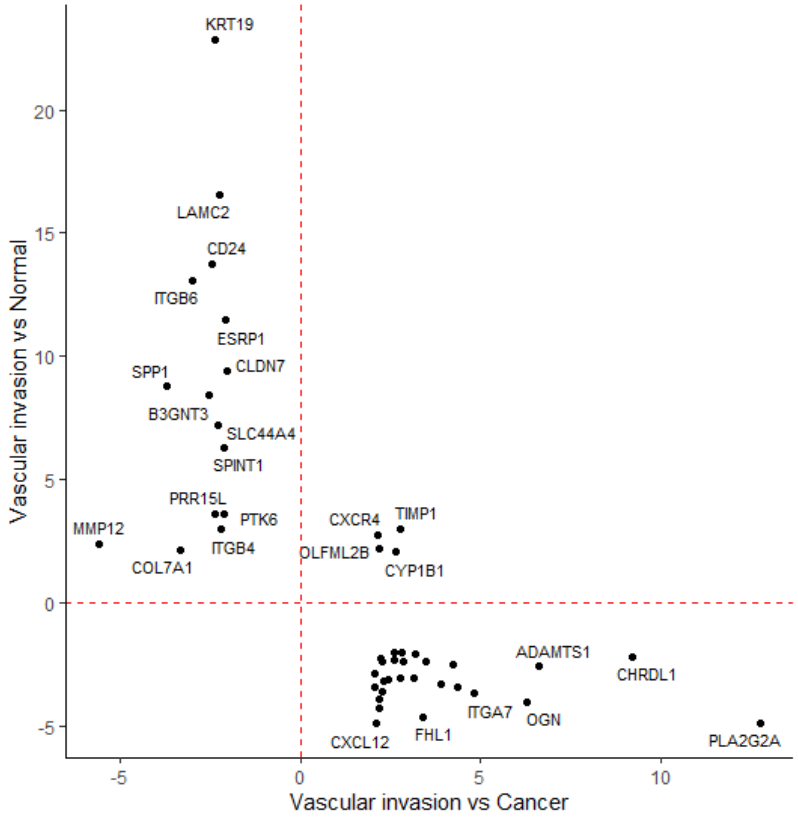

Figure 2. Scatter plot showing gene expression fold change of vascular invasion group (VI) compared to cancer (CA) and normal vessel (NV) group.

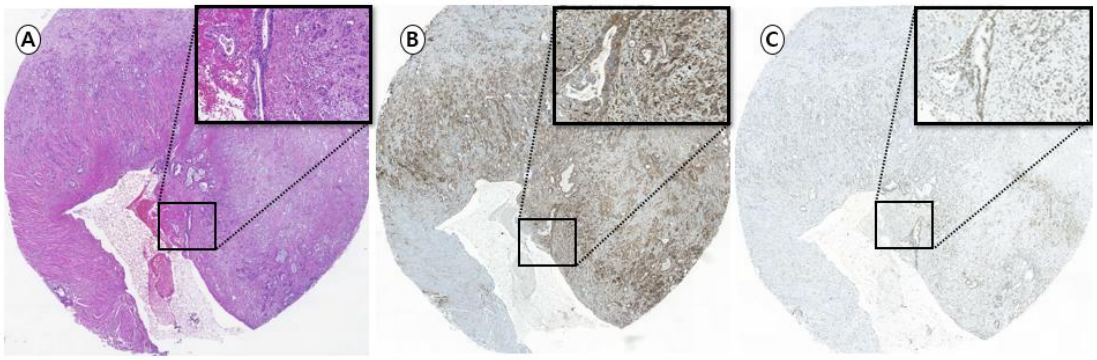

Figure 3 Representative images of portal/ superior mesenteric vein with cancer invasion **(A)** showing diffuse strong immunoreactivity for TIMP1 **(B)** and CXCR4 **(C)** (X2.3, X20 in inlet)

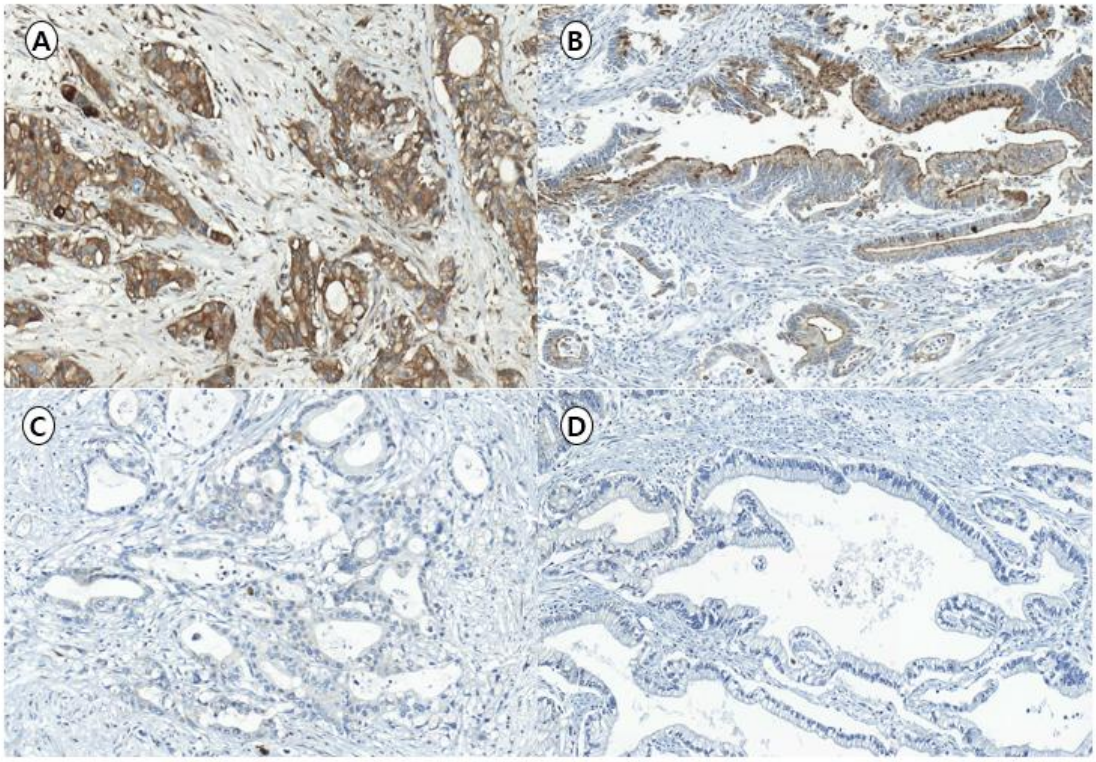

Figure 4 TIMP1 immunohistochemical (IHC) sections with different intensity (A) TIMP1 IHC intensity 3 (200×); (B) TIMP1 IHC intensity 2 (200×); (C) TIMP1 IHC intensity 1 (200×); (D) TIMP1 IHC intensity 0 (200×). TIMP1 IHC intensity 2 and 3 were classified as TIMP1 strong, and TIMP1 IHC intensity of 1 and 0 were classified as TIMP1 weak.

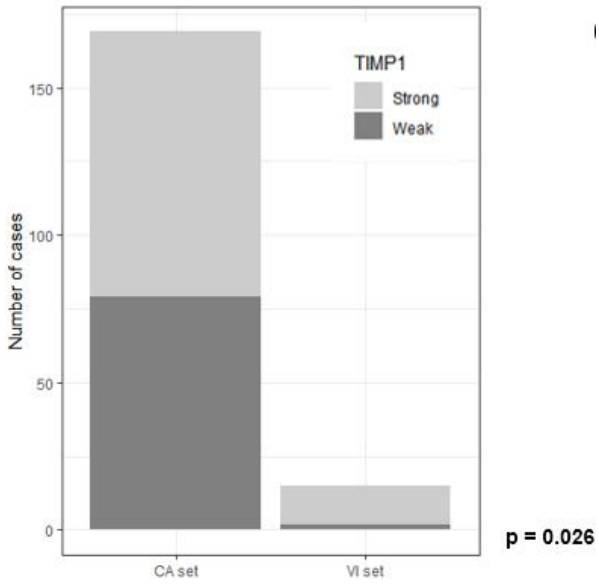

Figure 5. Number of strong TIMP1-expression cases in VI and CA set. The proportion of strong TIMP1-expression cases in the VI set is 86.7% (13/15), which is higher than the CA set (45%, 9/20)

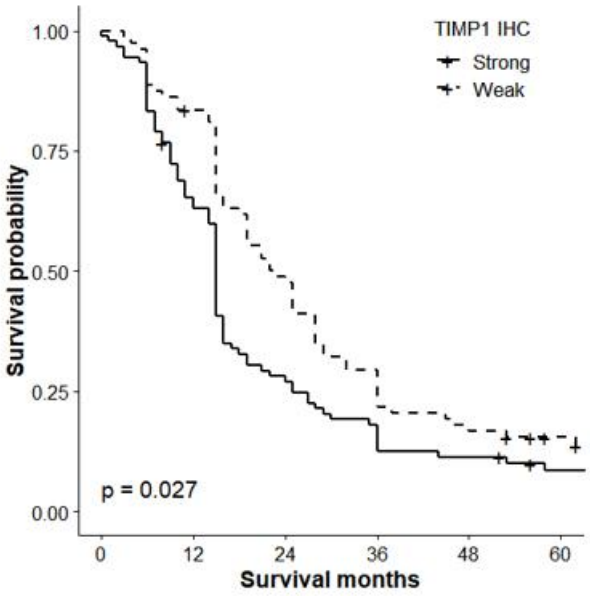

Figure 6. Overall survival according to TIMP1 status (5-year overall survival rate: TIMP1 strong, 8.6%; TIMP1 weak, 15.4%; P = 0.027).

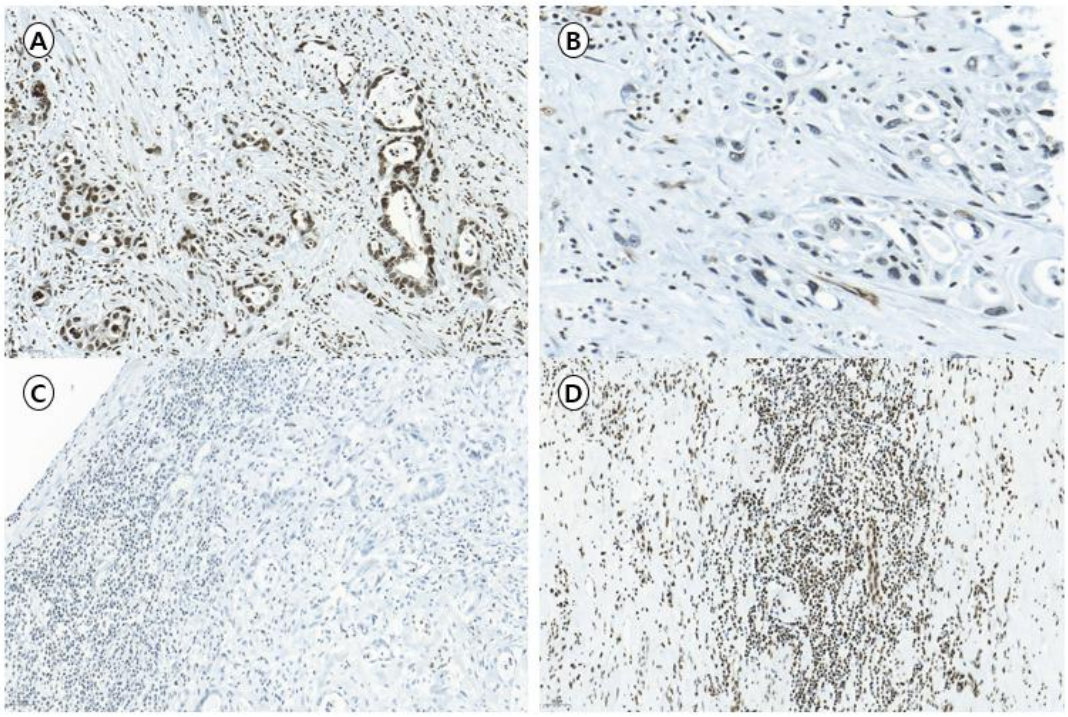

Figure 7. CXCR4 immunohistochemical (IHC) sections with different scores in tumor, inflammatory, and stromal cells. (A) CXCR4 IHC score 2, in tumor, inflammatory and, stromal cells (200×); (B) CXCR4 IHC score 1 in tumor cells, (400×); (C) CXCR4 IHC score 0 in tumor and stromal cells and CXCR4 IHC score 1 in inflammatory cells. (200×); (D) CXCR4 IHC score 2 in inflammatory cells (400×).

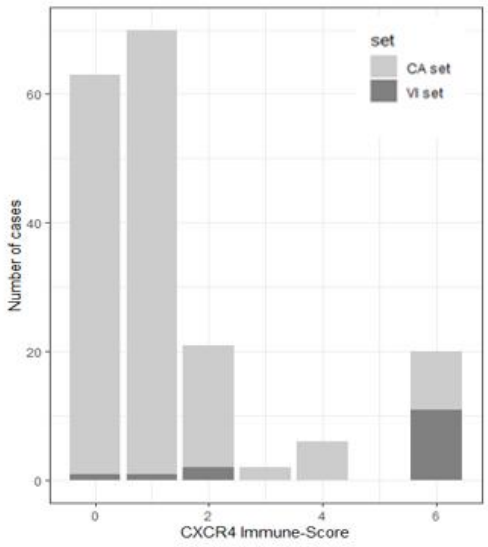

Figure 8. Number of cases for each CXCR4 immune-score in VI and CA set. The proportion of VI set in the immune-score 6 is 55% (11/20), which is higher than the CA set (45%, 9/20)

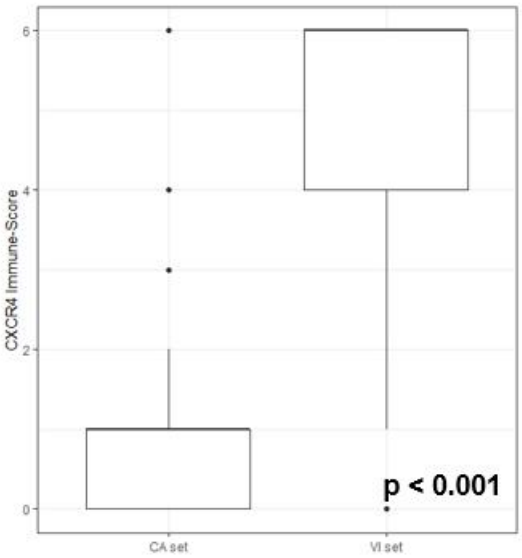

Figure 9. Box-plot of CXCR4 Immune-score in CA and VI set. The immune-score of the VI set (4.73±2.22) is higher than that of CA set (1.14±1.48, p value<0.001)

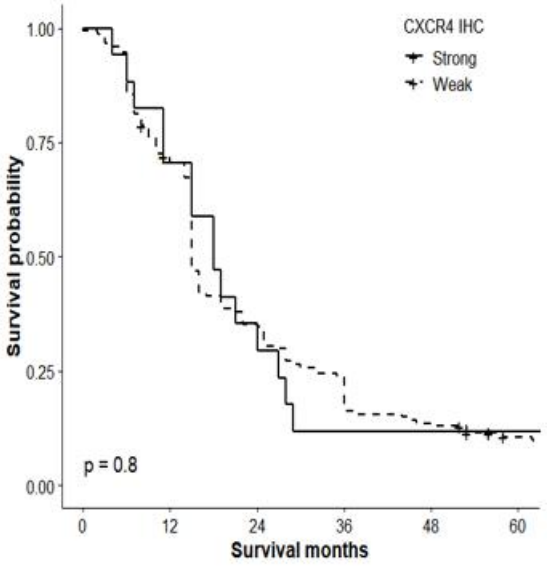

Figure 10. Overall survival according to CXCR4 expression status (5-year overall survival rate: CXCR4 strong, 11.8%; CXCR4 weak, 10.6%; P = 0.8).

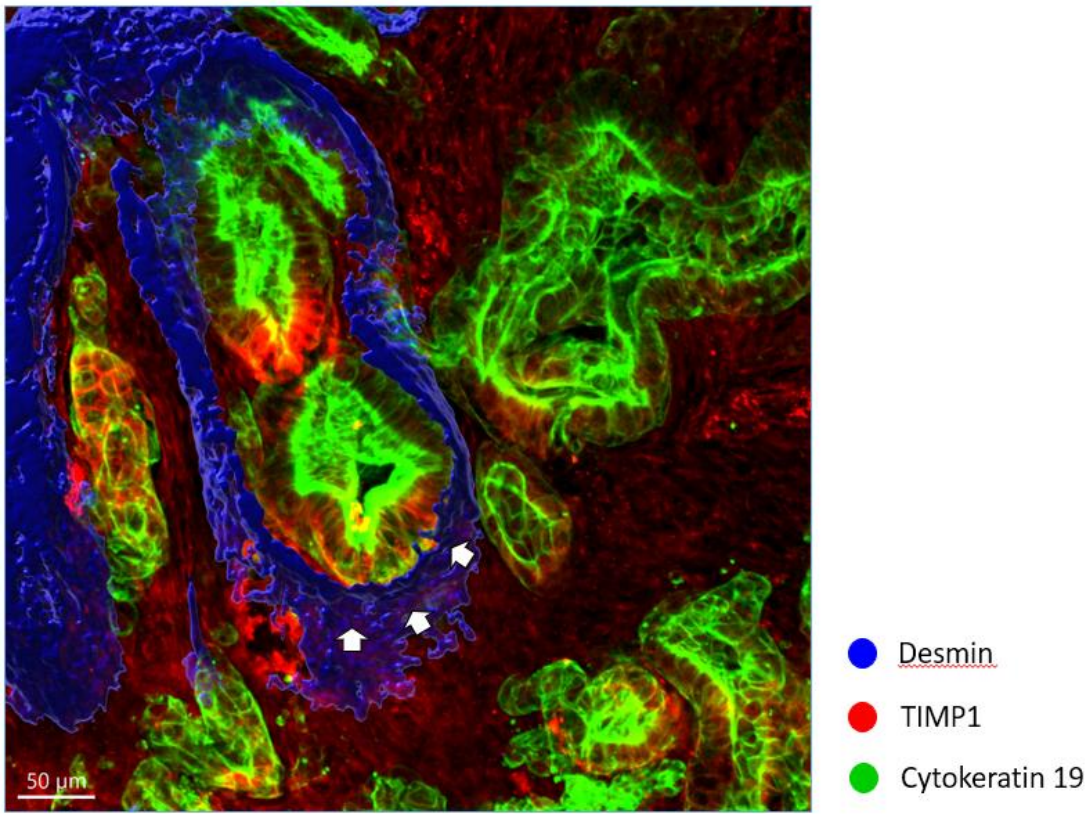

Figure 11. Representative image of multicolor immunofluorescent labeling of pancreatic ductal adenocarcinoma tissue with vascular invasion. TIMP1 expression (Red) is well observed in tubule forming cancer cells (Green) inside the vein (Blue)

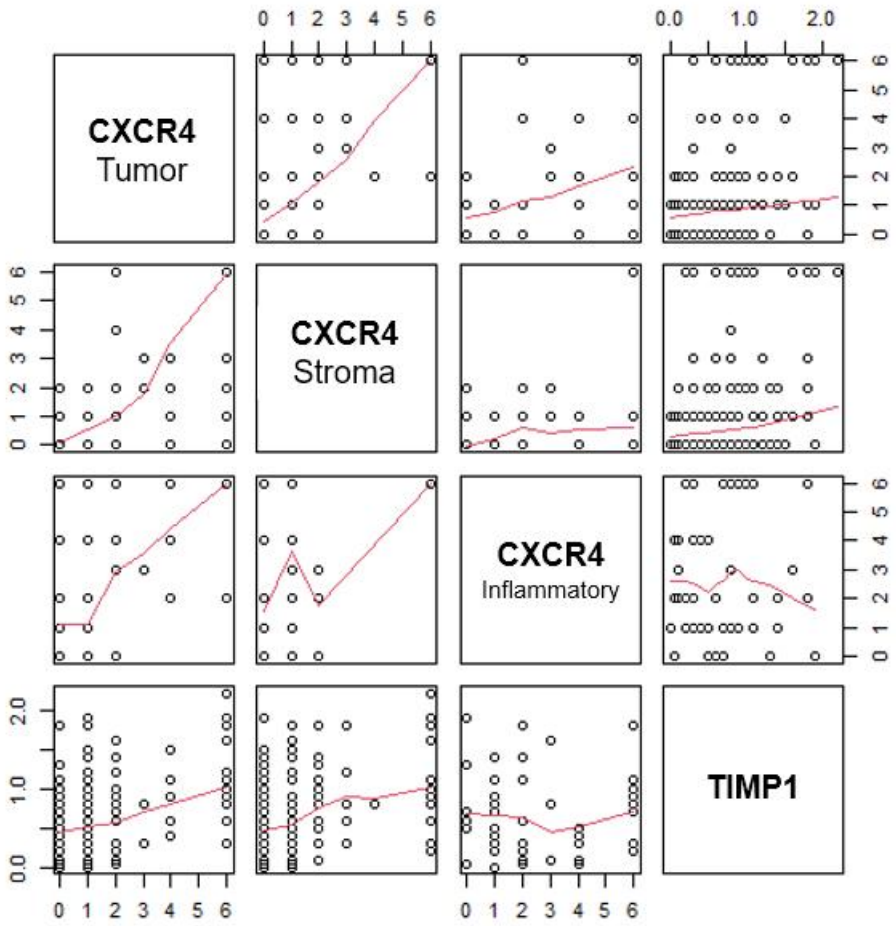

Figure 12. Scatter plot showing association between CXCR4 (tumor, stroma, and inflammatory cells) and TIMP1 using immune-score (IS). There is a correlation between IS of CXCR4 tumor, stroma, and inflammatory cells with correlation coefficients of 0.79, 0.52, and 0.53 respectively. And there is no significant correlation between IS of TIMP1 and CXCR4 (tumor, stroma, and inflammatory cells).

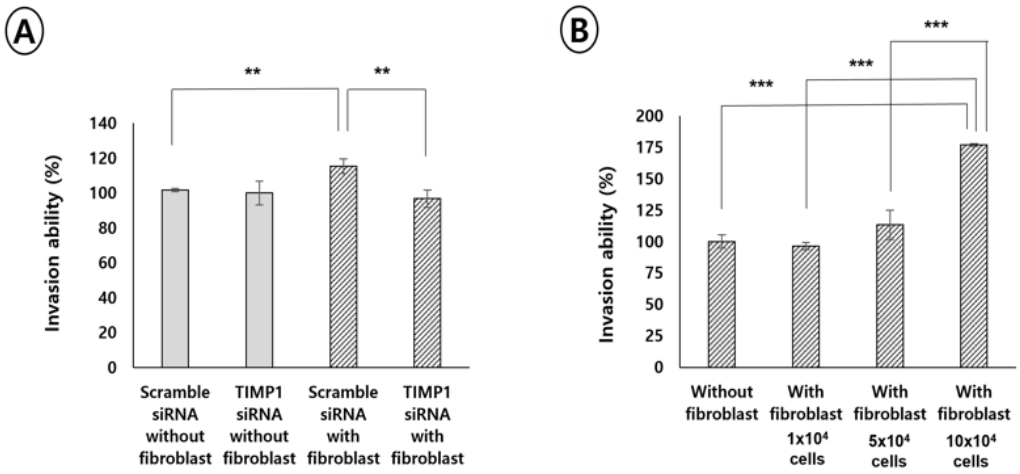

Figure 13. Invasion ability assay by boyden chamber system. (A) Inhibition of TIMP1 by siRNA reduced Panc1 cell invasion ability in the presence of CAF. (B) The effect of the CAF cell count in invasion ability. Cancer cell invasion ability increased as the number of CAF increased.

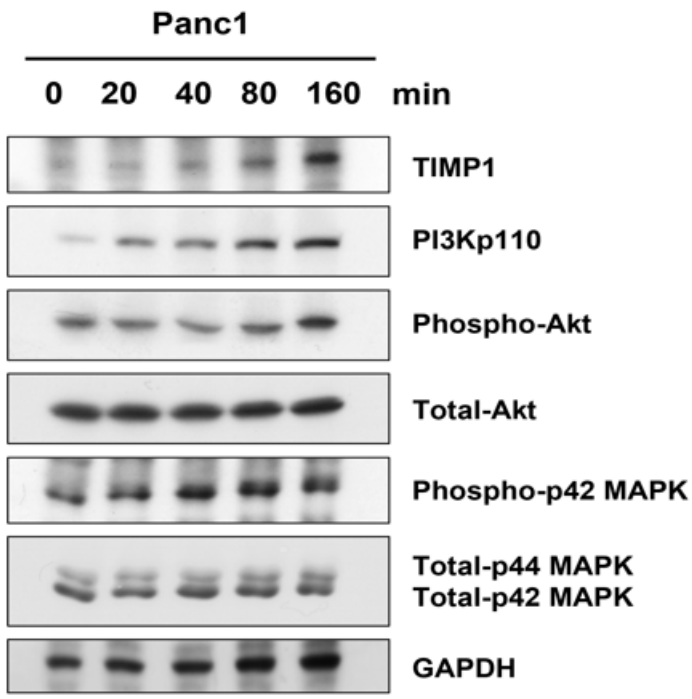

Figure 14 Western blot analysis in co-culture condition. Expression of TIMP1 increased along with PI3Kp110, phospho-AKT, and phospho-p42 MAPK as co-incubation time increased. While total Akt and p44/42 MAPK expression remained unchanged. GAPDH was used as loading control.

Discussion

In this study, TIMP1 was selected as a responsible gene involved in the large venous wall invasion of PDAC by utilizing gene expression array. Furthermore, protein validation was conducted with independent cohort and revealed that the lymphovascular invasion is more frequently observed in the strong TIMP1-expression group than in the weak TIMP1-expression group, which was also associated with lower overall survival rate.

Tissue inhibitor of metalloproteinase 1 (TIMP1) is a pleiotropic extracellular protein belonging to the TIMP family along with TIMP2, 3, and 4 (22, 23). TIMP1 was initially known to inhibit cancer invasion or metastasis as an inhibitor of MMP (24-26). However, several recent studies have revealed the ability of TIMP1 to regulate angiogenesis, epithelial-mesenchymal transition, and cell proliferation independent of its MMP inhibitory function (23, 24, 27, 28). Especially, the relationship between TIMP1 overexpression and poor prognosis has been revealed in several malignancies, such as breast (29, 30), colon (28, 31, 32), stomach (33-35), lung (36, 37), kidney (38), liver (39), and endometrium (40), and malignant melanomas (41, 42). In most studies, public data such as TCGA or Oncomine was used to verify the association between TIMP1 mRNA expression and unfavorable prognosis(28, 31, 38, 42). Additionally functional studies were conducted through western blot and invasion assay. In some studies, protein validation was performed through IHC using IS, such as multiplying or adding IHC intensity and area(28, 34, 39).

However, in the PDAC, other than some studies indicating that TIMP1 in serum or urine has a diagnostic value for detecting pancreatic malignancy (43, 44), there has been no study confirming TIMP1 expression in tissue analyzing its clinical significance or prognostic importance of the PDACs. As there is no standard scoring system to evaluate TIMP1 IHC expression, comparable to approaches of multiplying or adding IHC intensity used in previous studies conducted on other organs (28, 39), we evaluated both intensity and extent of TIMP1 expression

semi-quantitatively. Our result showed strong TIMP1 expression was more commonly noted in VI set than CA set. The frequency of lymphovascular invasion was higher in strong TIMP1-expression group than in the weak TIMP1-expression group, suggesting that TIMP1 may play a role in large venous wall invasion in PDAC, which is consistent with previous reports about TIMP1 as an oncogene in cancers from other organs.

CXCR4, which was also selected as a candidate gene related to large venous wall invasion through gene expression array, is a chemokine receptor subfamily (45). Several studies in colon (46, 47), and stomach (48) cancers showed association between the nuclear CXCR4 expression and worse survival. However, there were several studies with conflicting results. Spano et al described that the nuclear CXCR4 expression leads to better prognosis (49), while Nikkhoo B et al and Salvucci O et al suggested that cytoplasmic CXCR4 expression is an important for prognosis (50, 51). Additionally, some studies demonstrated that CXCR4 expression is associated with worse prognosis regardless of the expression pattern (52-54). These conflicting results might be due to variation of anbibody, interpretation of the staining, and heterogenous tumor types.

In this study, CXCR4 nuclear expression in VI group was higher than that of CA group. However, statistically relevant clinicopathologic feature was not observed including patient survival. We observed a few cases with both cytoplasmic and nuclear CXCR4 or cytoplasmic CXCR4 expression in tumor cells (19/167, 11.4%). Most showed focal and weak positivity, and its significant statistical difference with clinicopathologic feature and prognosis did not find.

Although there was no direct relationship between TIMP1 and CXCR4 in the molecular pathway, they might have overlapped or complementary roles in regulating cell migration and invasion depending on the specific cellular context. For example, TIMP1 may regulate the activity of metalloproteinases, which can activate CXCL12, leading to activation of the CXCL12/CXCR4 pathway and increased cell migration (38, 55). As such, both TIMP1 and CXCR4 are involved in

cell migration and invasion, we analyzed the relationship between TIMP1 and CXCR4, but did not find any correlation.

Invasion ability of TIMP1 on venous wall in PDAC only affect when Panc1 co-cultured with CAF. This suggests that CAF play an important role in the TIMP1-induced invasion pathway in PDAC. In addition, our western blot analysis revealed increased TIMP1 expression along with PI3Kp110, phospho-AKT, and phospho-p42 MAPK. This finding is consistent with previous reports on the relationship between TIMP1 and PI3K/Akt or MAPK pathways in various cancers (28, 56-59),. Therefore, TIMP1 expression in PDAC with venous invasion may be induced by activating PI3K/Akt and MAPK signaling pathway.

In conclusion, the present study identified TIMP1 as a biomarker for venous invasion of PDAC and has shown that the TIMP1/PI3K/Akt pathway play a role in the process of venous invasion. These findings provide valuable insights for TIMP1 signaling as a promising molecular target preventing venous wall invasion for patients with PDAC.

References

1. Committee of the Korean clinical practice guideline for pancreatic c, National Cancer Center K. Korean clinical practice guideline for pancreatic cancer 2021: A summary of evidence-based, multi-disciplinary diagnostic and therapeutic approaches. Pancreatology. 2021;21(7):1326-41.

2. Sohn TA, Yeo CJ, Cameron JL, Koniaris L, Kaushal S, Abrams RA, et al. Resected adenocarcinoma of the pancreas-616 patients: results, outcomes, and prognostic indicators. J Gastrointest Surg. 2000;4(6):567-79.

3. Schnelldorfer T, Ware AL, Sarr MG, Smyrk TC, Zhang L, Qin R, et al. Long-term survival after pancreatoduodenectomy for pancreatic adenocarcinoma: is cure possible? Ann Surg. 2008;247(3):456-62.

4. House MG, Gonen M, Jarnagin WR, D'Angelica M, DeMatteo RP, Fong Y, et al. Prognostic significance of pathologic nodal status in patients with resected pancreatic cancer. J Gastrointest Surg. 2007;11(11):1549-55.

5. Lim JE, Chien MW, Earle CC. Prognostic factors following curative resection for pancreatic adenocarcinoma: a population-based, linked database analysis of 396 patients. Ann Surg. 2003;237(1):74-85.

6. Nakao A, Harada A, Nonami T, Kaneko T, Takagi H. Clinical significance of carcinoma invasion of the extrapancreatic nerve plexus in pancreatic cancer. Pancreas. 1996;12(4):357-61.

7. Strobel O, Hank T, Hinz U, Bergmann F, Schneider L, Springfeld C, et al. Pancreatic Cancer Surgery: The New R-status Counts. Ann Surg. 2017;265(3):565-73.

8. Wang J, Lyu SC, Zhou L, Wang H, Pan F, Jiang T, et al. Prognostic analysis of pancreatic carcinoma with portal system invasion following curative resection. Gland Surg. 2021;10(1):35-49.

9. Fukuda S, Oussoultzoglou E, Bachellier P, Rosso E, Nakano H, Audet M, et al. Significance of the depth of portal vein wall invasion after curative resection for pancreatic adenocarcinoma. Arch Surg. 2007;142(2):172-9; discussion 80.

10. Wang J, Estrella JS, Peng L, Rashid A, Varadhachary GR, Wang H, et al. Histologic

tumor involvement of superior mesenteric vein/portal vein predicts poor prognosis in patients with stage Ⅱ pancreatic adenocarcinoma treated with neoadjuvant chemoradiation. Cancer. 2012;118(15):3801-11.

11. Hruban RH, Gaida MM, Thompson E, Hong SM, Noe M, Brosens LA, et al. Why is pancreatic cancer so deadly? The pathologist's view. J Pathol. 2019;248(2):131-41.

12. Li H, Pan W, Xu L, Yin D, Cheng S, Zhao F. Prognostic Significance of Microvascular Invasion in Pancreatic Ductal Adenocarcinoma: A Systematic Review and Meta-Analysis. Med Sci Monit. 2021;27:e930545.

13. Shin J, Wood LD, Hruban RH, Hong SM. Desmin and CD31 immunolabeling for detecting venous invasion of the pancreatobiliary tract cancers. PLoS One. 2020;15(11):e0242571.

14. Hong SM, Goggins M, Wolfgang CL, Schulick RD, Edil BH, Cameron JL, et al. Vascular invasion in infiltrating ductal adenocarcinoma of the pancreas can mimic pancreatic intraepithelial neoplasia: a histopathologic study of 209 cases. Am J Surg Pathol. 2012;36(2):235-41.

15. Hong SM, Jung D, Kiemen A, Gaida MM, Yoshizawa T, Braxton AM, et al. Three-dimensional visualization of cleared human pancreas cancer reveals that sustained epithelial-to-mesenchymal transition is not required for venous invasion. Mod Pathol. 2020;33(4):639-47.

16. Krishnan MS, Rajan Kd A, Park J, Arjunan V, Garcia Marques FJ, Bermudez A, et al. Genomic Analysis of Vascular Invasion in HCC Reveals Molecular Drivers and Predictive Biomarkers. Hepatology. 2021;73(6):2342-60.

17. Zhang R, Ye J, Huang H, Du X. Mining featured biomarkers associated with vascular invasion in HCC by bioinformatics analysis with TCGA RNA sequencing data. Biomed Pharmacother. 2019;118:109274.

18. Mannelqvist M, Stefansson IM, Bredholt G, Hellem Bo T, Oyan AM, Jonassen I, et al. Gene expression patterns related to vascular invasion and aggressive features in endometrial cancer. Am J Pathol. 2011;178(2):861-71.

19. Aljohani AI, Toss MS, Green AR, Rakha EA. The clinical significance of cyclin B1 (CCNB1) in invasive breast cancer with emphasis on its contribution to lymphovascular

invasion development. Breast Cancer Res Treat. 2023;198(3):423-35.

20. Zhang L, Wang Z, Li M, Sun P, Bai T, Wang W, et al. HCG18 Participates in Vascular Invasion of Hepatocellular Carcinoma by Regulating Macrophages and Tumor Stem Cells. Front Cell Dev Biol. 2021;9:707073.

21. Jung D, Shin J, Park J, Shin J, Sung YN, Kim Y, et al. Frequent Intraluminal Growth of Large Muscular Veins in Surgically Resected Colorectal Cancer Tissues: A 3-Dimensional Pathologic Reconstruction Study. Mod Pathol. 2023;36(3):100082.

22. Justo BL, Jasiulionis MG. Characteristics of TIMP1, CD63, and beta1-Integrin and the Functional Impact of Their Interaction in Cancer. Int J Mol Sci. 2021;22(17).

23. Moore CS, Crocker SJ. An alternate perspective on the roles of TIMPs and MMPs in pathology. Am J Pathol. 2012;180(1):12-6.

24. D'Angelo RC, Liu XW, Najy AJ, Jung YS, Won J, Chai KX, et al. TIMP-1 via TWIST1 induces EMT phenotypes in human breast epithelial cells. Mol Cancer Res. 2014;12(9):1324-33.

25. Ikenaka Y, Yoshiji H, Kuriyama S, Yoshii J, Noguchi R, Tsujinoue H, et al. Tissue inhibitor of metalloproteinases-1 (TIMP-1) inhibits tumor growth and angiogenesis in the TIMP-1 transgenic mouse model. Int J Cancer. 2003;105(3):340-6.

26. Forough R, Koyama N, Hasenstab D, Lea H, Clowes M, Nikkari ST, et al. Overexpression of tissue inhibitor of matrix metalloproteinase-1 inhibits vascular smooth muscle cell functions in vitro and in vivo. Circ Res. 1996;79(4):812-20.

27. Jung KK, Liu XW, Chirco R, Fridman R, Kim HR. Identification of CD63 as a tissue inhibitor of metalloproteinase-1 interacting cell surface protein. EMBO J. 2006;25(17):3934-42.

28. Song G, Xu S, Zhang H, Wang Y, Xiao C, Jiang T, et al. TIMP1 is a prognostic marker for the progression and metastasis of colon cancer through FAK-PI3K/AKT and MAPK pathway. J Exp Clin Cancer Res. 2016;35(1):148.

29. Wurtz SO, Schrohl AS, Mouridsen H, Brunner N. TIMP-1 as a tumor marker in breast cancer--an update. Acta Oncol. 2008;47(4):580-90.

30. Schrohl AS, Holten-Andersen MN, Peters HA, Look MP, Meijer-van Gelder ME, Klijn JG, et al. Tumor tissue levels of tissue inhibitor of metalloproteinase-1 as a

prognostic marker in primary breast cancer. Clin Cancer Res. 2004;10(7):2289-98.

31. Huang R, Wang K, Gao L, Gao W. TIMP1 Is A Potential Key Gene Associated With The Pathogenesis And Prognosis Of Ulcerative Colitis-Associated Colorectal Cancer. Onco Targets Ther. 2019;12:8895-904.

32. Lee JH, Choi JW, Kim YS. Plasma or serum TIMP-1 is a predictor of survival outcomes in colorectal cancer: a meta-analysis. J Gastrointestin Liver Dis. 2011;20(3):287-91.

33. Wang YY, Li L, Zhao ZS, Wang HJ. Clinical utility of measuring expression levels of KAP1, TIMP1 and STC2 in peripheral blood of patients with gastric cancer. World J Surg Oncol. 2013;11:81.

34. Liu H, Xiang Y, Zong QB, Zhang XY, Wang ZW, Fang SQ, et al. miR-6745-TIMP1 axis inhibits cell growth and metastasis in gastric cancer. Aging (Albany NY). 2021;13(21):24402-16.

35. Grunnet M, Mau-Sorensen M, Brunner N. Tissue inhibitor of metalloproteinase 1 (TIMP-1) as a biomarker in gastric cancer: a review. Scand J Gastroenterol. 2013;48(8):899-905.

36. Gouyer V, Conti M, Devos P, Zerimech F, Copin MC, Creme E, et al. Tissue inhibitor of metalloproteinase 1 is an independent predictor of prognosis in patients with nonsmall cell lung carcinoma who undergo resection with curative intent. Cancer. 2005;103(8):1676-84.

37. Fong KM, Kida Y, Zimmerman PV, Smith PJ. TIMP1 and adverse prognosis in non-small cell lung cancer. Clin Cancer Res. 1996;2(8):1369-72.

38. Shou Y, Liu Y, Xu J, Liu J, Xu T, Tong J, et al. TIMP1 Indicates Poor Prognosis of Renal Cell Carcinoma and Accelerates Tumorigenesis via EMT Signaling Pathway. Front Genet. 2022;13:648134.

39. Song T, Dou C, Jia Y, Tu K, Zheng X. TIMP-1 activated carcinoma-associated fibroblasts inhibit tumor apoptosis by activating SDF1/CXCR4 signaling in hepatocellular carcinoma. Oncotarget. 2015;6(14):12061-79.

40. Honkavuori M, Talvensaari-Mattila A, Puistola U, Turpeenniemi-Hujanen T, Santala M. High serum TIMP-1 is associated with adverse prognosis in endometrial

carcinoma. Anticancer Res. 2008;28(5A):2715-9.

41. Toricelli M, Melo FHM, Hunger A, Zanatta D, Strauss BE, Jasiulionis MG. Timp1 Promotes Cell Survival by Activating the PDK1 Signaling Pathway in Melanoma. Cancers (Basel). 2017;9(4).

42. Wang P, Yang X, Zhou N, Wang J, Li Y, Liu Y, et al. Identifying a Potential Key Gene, TIMP1, Associated with Liver Metastases of Uveal Melanoma by Weight Gene Co-Expression Network Analysis. Onco Targets Ther. 2020;13:11923-34.

43. Slater EP, Fendrich V, Strauch K, Rospleszcz S, Ramaswamy A, Matthai E, et al. LCN2 and TIMP1 as Potential Serum Markers for the Early Detection of Familial Pancreatic Cancer. Transl Oncol. 2013;6(2):99-103.

44. Roy R, Zurakowski D, Wischhusen J, Frauenhoffer C, Hooshmand S, Kulke M, et al. Urinary TIMP-1 and MMP-2 levels detect the presence of pancreatic malignancies. Br J Cancer. 2014;111(9):1772-9.

45. Jacobson O, Weiss ID. CXCR4 chemokine receptor overview: biology, pathology and applications in imaging and therapy. Theranostics. 2013;3(1):1-2.

46. Speetjens FM, Liefers GJ, Korbee CJ, Mesker WE, van de Velde CJ, van Vlierberghe RL, et al. Nuclear localization of CXCR4 determines prognosis for colorectal cancer patients. Cancer Microenviron. 2009;2(1):1-7.

47. Wang SC, Lin JK, Wang HS, Yang SH, Li AF, Chang SC. Nuclear expression of CXCR4 is associated with advanced colorectal cancer. Int J Colorectal Dis. 2010;25(10):1185-91.

48. Masuda T, Nakashima Y, Ando K, Yoshinaga K, Saeki H, Oki E, et al. Nuclear expression of chemokine receptor CXCR4 indicates poorer prognosis in gastric cancer. Anticancer Res. 2014;34(11):6397-403.

49. Spano JP, Andre F, Morat L, Sabatier L, Besse B, Combadiere C, et al. Chemokine receptor CXCR4 and early-stage non-small cell lung cancer: pattern of expression and correlation with outcome. Ann Oncol. 2004;15(4):613-7.

50. Nikkhoo B, Jalili A, Fakhari S, Sheikhesmaili F, Fathi F, Rooshani D, et al. Nuclear pattern of CXCR4 expression is associated with a better overall survival in patients with gastric cancer. J Oncol. 2014;2014:808012.

51. Salvucci O, Bouchard A, Baccarelli A, Deschenes J, Sauter G, Simon R, et al. The role of CXCR4 receptor expression in breast cancer: a large tissue microarray study. Breast Cancer Res Treat. 2006;97(3):275-83.

52. Kato M, Kitayama J, Kazama S, Nagawa H. Expression pattern of CXC chemokine receptor-4 is correlated with lymph node metastasis in human invasive ductal carcinoma. Breast Cancer Res. 2003;5(5):R144-50.

53. Li YM, Pan Y, Wei Y, Cheng X, Zhou BP, Tan M, et al. Upregulation of CXCR4 is essential for HER2-mediated tumor metastasis. Cancer Cell. 2004;6(5):459-69.

54. Wang N, Wu QL, Fang Y, Mai HQ, Zeng MS, Shen GP, et al. Expression of chemokine receptor CXCR4 in nasopharyngeal carcinoma: pattern of expression and correlation with clinical outcome. J Transl Med. 2005;3:26.

55. Jackson HW, Defamie V, Waterhouse P, Khokha R. TIMPs: versatile extracellular regulators in cancer. Nat Rev Cancer. 2017;17(1):38-53.

56. Zhang J, Wang J, Yue K, Li P, Shen W, Qiao X, et al. FAM83B promotes the invasion of primary lung adenocarcinoma via PI3K/AKT/NF-kappaB pathway. BMC Pulm Med. 2023;23(1):32.

57. Wang L, Wang J, Chen L. TIMP1 represses sorafenib-triggered ferroptosis in colorectal cancer cells by activating the PI3K/Akt signaling pathway. Immunopharmacol Immunotoxicol. 2023:1-7.

58. Tian Z, Tan Y, Lin X, Su M, Pan L, Lin L, et al. Arsenic trioxide sensitizes pancreatic cancer cells to gemcitabine through downregulation of the TIMP1/PI3K/AKT/mTOR axis. Transl Res. 2023;255:66-76.

59. Su Y, Wan D, Song W. Dryofragin inhibits the migration and invasion of human osteosarcoma U2OS cells by suppressing MMP-2/9 and elevating TIMP-1/2 through PI3K/AKT and p38 MAPK signaling pathways. Anticancer Drugs. 2016;27(7):660-8.

국문요약

연구배경 및 목적

췌장선암은 우리나라에서 8 번째로 흔한 암으로 5 년 전체 생존율이 약 12.2%로 낮다. 정맥 침범이 예후 불량의 원인으로 알려져 있지만 이에 대한 정확한 매커니즘은 아직 제대로 알려져 있지 않다. 해당 매커니즘을 더 명확하게 이해하기 위해 Gene expression array 를 이용해서 췌장선암에서 정맥 침범과 관련한 바이오마커를 발굴하고, 단백질 발현을 검증한 후, 그 매커니즘을 이해하는 기능 연구를 진행하였다.

연구재료와 연구방법

췌장선암을 진단받고 수술을 진행한 8 개의 FFPE 조직을 수집하였다. 이후, gene expression array 를 시행하기 위해 다음 세 그룹에 따라 micro-dissection 을 시행하였다. 1) 간문맥/상간막정맥에 암세포 침입이 있는 그룹 (VI), 2) 간문맥/상간맥정맥이 없는 암세포 조직 (CA), 3) 정상 간문맥/상간막정맥 조직 (NV). 후보 유전자의 단백질 발현은 면역조직화학 염색 후 2D 이미지를 통해 220 케이스에서 검증하였고, 추가로 tissue clearing 과 multiple immunofluorescence labeling 을 이용하여 3D 이미지로도 검증하였다. 췌장선암 정맥침윤에서 잠재적 바이오마커의 역할을 확인하기 위해 인간 내피세포 (EA.hy926), 암관련 섬유아세포 (CAF), 그리고 췌장선암 세포주 (Panc 1) 을 이용하여 invasion assay 및 western blot 을 시행하였다.

연구결과

TIMP1, CXCR4, OLFML2B, CYP1B1 등 4 개의 유전자가 VI group 에서 CA, NV group 에 비해 특이적으로 높게 발현되었으며, VI set 의 TIMP1 ($p=0.026$)과 CXCR4 ($p<0.001$) 단백질 발현이 CA set 에 비해 유의하게 높았다. 또한 정맥침습

영역에서의 TIMP1 발현을 3D imaging 을 통해 확인하였다. TIMP1 발현이 강한 환자는 TIMP1 발현이 약한 환자에 비해 림프혈관침범의 빈도가 높았고 ($p<0.001$), 5 년 생존율은 더 낮았다($p=0.027$). Invasion assay 에서 siRNA 를 이용해서 TIMP1 발현을 억제 시켰을 때, CAF 가 있는 조건에서 암세포 침윤능력이 감소되었다. 정맥침범을 모방한 공동배양조건에서 Panc1 cell 내 TIMP1 발현이 시간이 흐름에 따라 증가하였으며 PI3Kp110 및 phospho-맛도 함께 증가하는 것을 western blot 에서 확인하였다.

결론

이번 연구 결과, 췌장선암의 정맥침범에서 바이오마커로 선정한 TIMP1 이 PI3K/Akt 과 MAPK 경로를 통해 정맥침범 process 에 작용할 수 있음을 확인하였고, 이는 정맥침범이 있는 췌장선암 환자의 molecular target 개발을 위한 기본 정보를 제공할 수 있다.